Charge compensated binding of divalent metals to bacterioferritin: H^+ release associated with cobalt(II) and zinc(II) binding at dinuclear metal sites

Nick E. Le Brun[a], Angus M. Keech[a], Marcia R. Mauk[b], A. Grant Mauk[b], Simon C. Andrews[c], Andrew J. Thomson[a], Geoffrey R. Moore[a,*]

[a] *Centre for Metalloprotein Spectroscopy and Biology, School of Chemical Sciences, University of East Anglia, Norwich NR4 7TJ, UK*
[b] *Department of Biochemistry and Molecular Biology, University of British Columbia, Vancouver, British Columbia V6T 1Z3, Canada*
[c] *The Krebs Institute, Department of Molecular Biology and Biotechnology, University of Sheffield, Sheffield S10 2UH, UK*

Received 26 July 1996; revised version received 7 October 1996

Abstract Divalent metal ion binding to the bacterial iron-storage protein, bacterioferritin (BFR), which contains a dinuclear metal binding site within each of its 24 subunits, was investigated by potentiometric and spectrophotometric methods. Cobalt(II) and zinc(II) were found to bind at both high- and low-affinity sites. Cobalt(II) binding at the high-affinity site was observed at a level of two per subunit with the release of ~1.6 protons per metal ion, thus confirming the dinuclear metal centre as the high-affinity site. Zinc(II) binding at the dinuclear centre (high-affinity site) resulted in the release of ~2 protons per metal ion, but exhibited a binding stoichiometry which indicated that not all dinuclear centres were capable of binding two zinc(II) ions. Competition data showed that binding affinities for the dinuclear centre were in the order zinc(II) > cobalt(II), and also confirmed the unexpected stoichiometry of zinc(II) binding. This work emphasises the importance of charge neutrality at the dinuclear centre.

Key words: Bacterioferritin; Dinuclear center; Cobalt(II); Zinc(II); Potentiometry; Charge neutrality

1. Introduction

Metal ion binding to proteins is often associated with the uptake or release of protons to provide charge compensation. Often there will be complete charge compensation so that the overall interaction is electroneutral. Transferrins are a particularly well-studied class of metal binding proteins in this respect [1–3]. Human serum transferrin binds two iron(III) ions at separate sites, each in concert with one HCO_3^- and releases a net six protons: one from each anion, which thus become CO_3^{2-}; and four from tyrosine side chains that bind to the iron(III) ions. Therefore, in this case metal binding is not fully charge compensated and there is a difference in the total charge of apo-transferrin and [Fe(III)-CO_3^{2-}]$_2$-transferrin that can be detected by electrophoresis of the native proteins. The reduction of the non-haem-iron(III) core of mammalian ferritin is another system which appears not to be fully charge compensated. Watt et al. [4] have shown that two protons are taken up per electron when the core iron(III) is reduced to iron(II).

We are interested in the formation and breakdown of dinuclear metal centres in proteins and in the present paper report potentiometric and spectroscopic studies of the binding of cobalt(II) and zinc(II) to the oligomeric non-haem-iron-containing cytochrome b_{557}, also known as bacterioferritin (BFR), from *Escherichia coli*. BFR is an iron-storage protein consisting of 24 identical subunits of M_r = 18 500 which pack together to form an approximately spherical molecule with a hollow centre in which large amounts of iron can be deposited as a ferric-oxy-hydroxide-phosphate mineral [5,6]. In addition to the iron core, BFR contains up to 12 *b*-type haem groups situated between symmetry-related subunit pairs, and ligated by two methionines (Met-52 and Met-52′) [7,8], and a dinuclear metal-binding site in each subunit called the ferroxidase centre [8–10]. The form of the centre when occupied by divalent metal ions is represented schematically in Fig. 1a, which reveals that the two metal ions are bridged by two carboxylates and that each has an additional, monodentate, carboxylate ligand and a histidine ligand. The mechanistic details of aerobic oxidative iron-uptake by BFR have not been fully determined but it has been established that the process involves at least three kinetically distinguishable phases: binding of iron(II) at the ferroxidase centre (phase 1); fast oxidation of iron(II) to iron(III) at the ferroxidase centre (phase 2); and subsequent formation of the mineral core (phase 3) [9,10]. Thus, the ferroxidase centre is proposed to play a key role in this process. Similar dinuclear metal centres are found in a range of proteins including the R2 subunit of ribonucleotide reductase (RNR) (Fig. 1b), and the hydroxylase subunit of methane monooxygenase [11–13]. A common feature to the chemistry of all these proteins is that their dinuclear centres react with O_2, though the nature of the overall reactions are different.

There is considerable interest in the mechanisms of action of proteins containing dinuclear iron centres, particularly in the structural bases of their mechanistic differences. The assembly and disassembly of these centres is also of interest and, at least in the case of BFR, may play a central role in the mechanism of reaction. Since the centres are invariably buried within 4-α-helical bundle structures the question of charge distribution within them is an important one. This is so not only for dinuclear centres undergoing redox change but also for the assembly of such centres. In the present paper we address this latter issue by investigating the binding of cobalt(II) and zinc(II) to BFR with unoccupied ferroxidase centres, i.e. apo-BFR. We chose these metal ions because they do not undergo redox reactions with BFR in the presence of O_2, and because previous work had indicated that both bind at the ferroxidase centres [10,14]. To investigate the degree of charge compensation we have determined the number of pro-

*Corresponding author. Fax: (44) (1603) 259396.
E-mail: g.moore@uea.ac.uk

PII S0014-5793(96)01172-6

tons released per metal ion bound by potentiometric titration. We conducted our studies at pH 6.0–6.5 to permit comparison of the results with the structure of the empty site of apo-RNR at pH 6.0 that was described by Åberg et al. [15]. The three-dimensional structure of apo-BFR has not been reported.

2. Materials and methods

Overexpression and purification of BFR [10], the removal of non-haem iron by treatment with sodium dithionite and 2,2-bipyridyl [16], and the determination of haem content by the pyridine haemochromagen method [17] were all carried out as previously described. The haem contents of the samples used for the experiments described in the present paper were 5–6 per 24 subunits, a typical value for recombinant BFR [10]. All concentrations of BFR given are for the assembled 24-mer.

The change in proton binding that is associated with metal binding to BFR was studied according to the method of Laskowski and Finkenstadt [18] with a Radiometer Model ABU93 titrator operated under computer control [19]. $CoCl_2$ and $ZnCl_2$ solutions were prepared gravimetrically by dilution of atomic absorption standards (Merck Tritisol) to known concentrations and ionic strength was adjusted to 0.1 M with KCl. Titrations were performed with unbuffered solutions of BFR (0.083–0.75 μM) in 0.1 M KCl and at 25°C. Potentiometric data were fitted with a model that assumes two types of independent metal binding site [20] and a stoichiometry of two of each type of site per BFR subunit.

Spectrophotometric experiments were carried out using a Hitachi 4001 spectrophotometer interfaced to a 486PC. Visible difference spectra were recorded with apo-BFR solutions in both reference and sample cuvettes, and with metal-containing solution added to the sample cuvette and an equal volume of water added to the reference cuvette. Solutions of $CoCl_2$ and $ZnCl_2$ were freshly prepared prior to each experiment by dissolving weighed amounts of the salts in AnalaR grade water. Microlitre additions of the metal ion solutions to optical cuvettes were made using a Hamilton micro-syringe. Each addition was followed by stirring and an incubation time of approx. 10 min. BFR (13.2 μM) was in 0.1 M MES buffer, pH 6.5. The dilution of the protein solutions during the titrations was minimised by using concentrated metal ion solutions. The resultant change in protein concentration (<4%) was not taken into account when fitting the data.

3. Results and discussion

3.1. Cobalt(II) binding to BFR

Fig. 2a shows the change in proton binding to BFR that occurs upon addition of cobalt(II) at pH 6.0. The data are well described by a model (solid line) in which two cobalt(II) ions bind at a dinuclear site with the release of 1.62 ± 0.02 protons per metal ion and apparent dissociation constant (K_d) values for each cobalt(II) ion of $1 \pm 0.1 \times 10^{-6}$ M. Previous spectroscopic experiments with wild-type and site-directed variants of BFR showed that cobalt(II) ions preferentially bind at the ferroxidase centre (2 cobalt(II) per centre) [14]. Binding of cobalt(II) ions at each ferroxidase centre was found to occur with macroscopic K_d values estimated to be of the order of $\sim 10^{-5}$ M. Individual microscopic K_d values were not obtained.

Further spectroscopic investigation of cobalt(II) binding was carried out in the present study. Fig. 3a shows the visible absorption difference spectra obtained on the addition of cobalt(II) to apo-BFR. Absorbance bands, due to cobalt(II) d-d transitions, were observed at the wavelengths 520, 555, 600 and 620 nm, with associated extinction coefficients of 126, 155, 107 and 75 M^{-1} cm^{-1} (per cobalt), respectively [14]. These energies and intensities are characteristic of pseudo-tetrahedral or penta-coordinate cobalt(II) complexes, consistent with cobalt(II) binding at the ferroxidase centre. Saturation

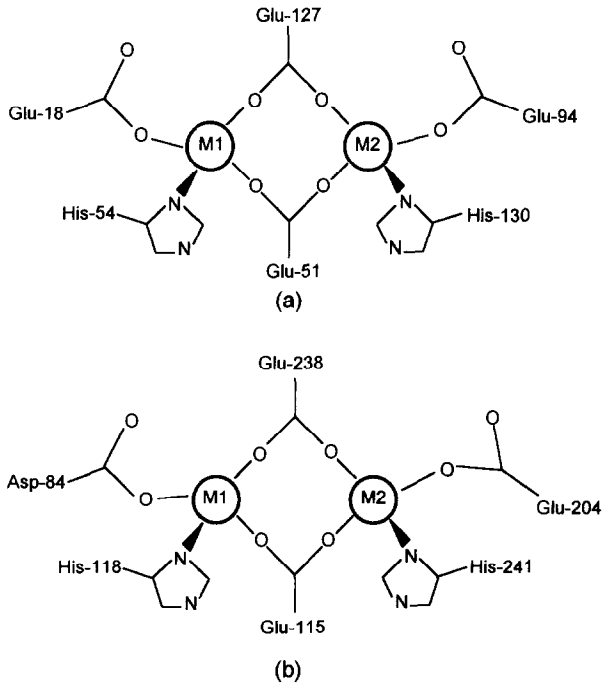

Fig. 1. Schematic representations of the dinuclear metal centres of BFR and the reduced form of the R2 protein of ribonucleotide reductase. (a) BFR. Adapted from [8]. Although the chemical nature and redox level of the occupying metal ions were not stated by Frolow et al. [8] it is likely that M1 and M2 are both Mn(II), since crystals of BFR were obtained from solutions of apo-BFR and 100 μM $MnCl_2$. (b) R2 RNR. Adapted from [12]. M1 and M2 are iron(II) ions.

occurs at a stoichiometry of ~50 cobalt(II) ions per BFR molecule (Fig. 3c). The data were fitted to a model (solid line) which assumes equivalent, non-interacting binding sites [14], and gave an estimate of the K_d value of $3.4 \pm 2.6 \times 10^{-6}$ M.

The spectroscopic data indicate that under the conditions of the potentiometric study, the occupancy of the dinuclear site with cobalt(II) ions will be >95% at a stoichiometry of 48 cobalt(II) ions per BFR molecule. The gradual increase in protons released as cobalt(II) is added at above stoichiometric levels is due to cobalt(II) binding at additional sites. Analysis of the potentiometric data indicates that two additional cobalt(II) ions bind per subunit with K_d values of $\sim 2 \times 10^{-4}$ M and with release of ~0.6 protons per cobalt(II) ion. These weakly bound cobalt(II) ions were not detected in the visible absorption spectroscopic study of Fig. 3 suggesting that they have very low extinction coefficients for their d-d transitions and are thus of octahedral symmetry. The parameters derived from fitting of the potentiometric titrations are summarised in Table 1.

3.2. Zinc(II) binding to BFR

Fig. 2b shows the change in proton binding to BFR that occurs upon addition of zinc(II) at pH 6.0. As observed for cobalt(II), binding of zinc(II) to BFR is accompanied by release of protons. The data in Fig. 2b could be fitted to a model (solid line) that assumes: (i) two zinc(II) ions bind at a high-affinity site; (ii) two zinc(II) ions bind at low-affinity sites; and, (iii) only 82% of available sites are able to bind zinc(II) at this pH.

The parameters derived from fitting the data to this model indicate that zinc(II) binds to the high-affinity site with an apparent K_d value of $1.09 \pm 0.09 \times 10^{-7}$ M, resulting in the release of 1.96 ± 0.01 protons for each zinc(II) ion bound, and that a further two zinc(II) ions bind at low-affinity sites with K_d values of $\sim 10^{-4}$ M and the release of 0.9 protons per zinc(II) bound. On increasing pH to 6.5 similar potentiometric data were obtained for zinc(II) binding (not shown) with the fitting model indicating that, for the high-affinity site, the K_d was increased by a factor of two, while the proton stoichiometry was little changed. For the low-affinity site, the K_d and proton stoichiometry were both increased by a factor of two (Table 1).

Previous work on the oxidative uptake of iron(II) by BFR showed that zinc(II) can bind to the ferroxidase centre resulting in the inhibition of iron(II) oxidation [10]. However, this previous study did not report binding affinities for zinc(II) and since zinc(II) does not have favourable spectroscopic properties for their determination we have investigated the relative binding affinities of zinc(II) and cobalt(II) in a competition experiment (Fig. 3).

Fig. 3b shows the change in the absorbance spectrum upon addition of zinc(II) to the saturated cobalt(II)-BFR complex. As the zinc(II) concentration is increased, the absorbance decreases sharply. This can be seen most clearly in the plot of Fig. 3c which shows that the initial gradient of the absorbance increase as cobalt(II) is added is less than the initial gradient of the absorbance decrease as zinc(II) is added, even though there is a 50% excess of cobalt(II) over the ferroxidase metal

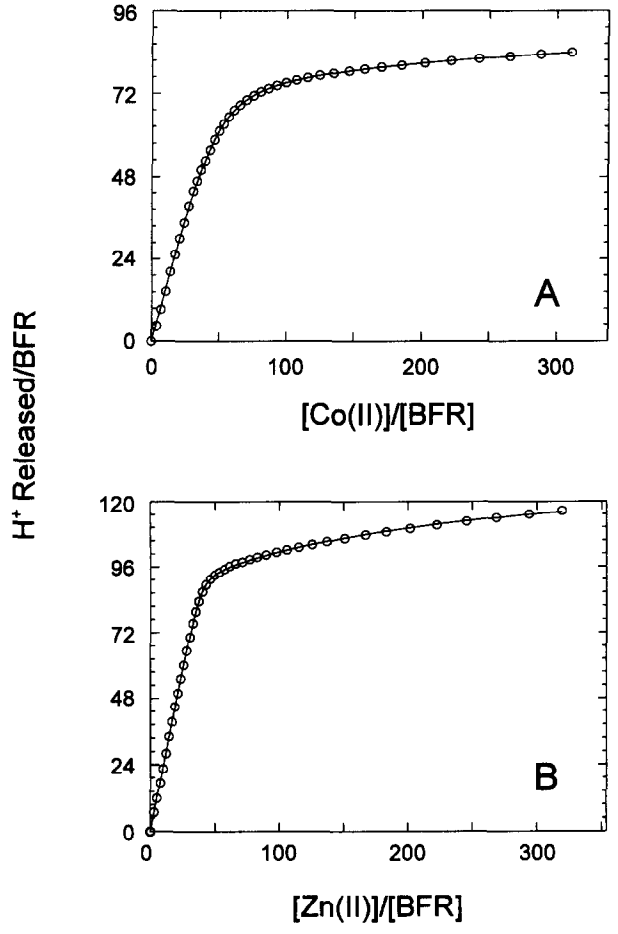

Fig. 2. The change in proton binding observed upon titration of BFR with divalent metal ions (25°C, $\mu = 0.1$ M): (A) $CoCl_2$; $[BFR]_{initial} = 0.362$ μM, pH 5.97. (B) $ZnCl_2$; $[BFR]_{initial} = 0.366$ μM, pH 5.98. In each case, the solid line is a non-linear least squares fit to the data calculated as described in the text.

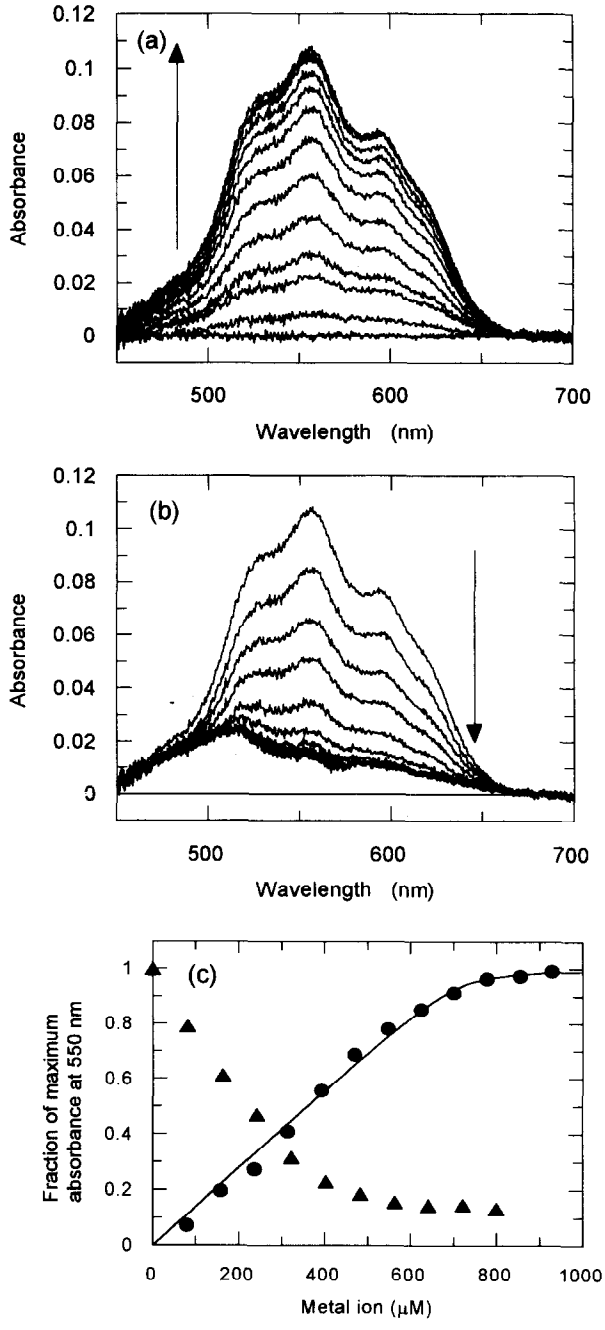

Fig. 3. Optical titrations of apo-BFR with solutions of cobalt(II) and zinc(II) chlorides. Apo-BFR (13.2 μM) was in 0.1 M MES buffer pH 6.5. (a) Visible difference spectra recorded after the addition of each aliquot of cobalt(II) to apo-BFR as described in Section 2. (b) Visible difference spectra recorded after the addition of each aliquot of zinc(II) to apo-BFR solution containing cobalt(II) (930 μM). (c) Change in absorbance with increasing concentrations of cobalt(II) (●, 0–930 μM) or zinc(II) (▲, 930 μM cobalt(II), 0–790 μM). The shape of the zinc(II) curve indicates that zinc(II) displaces cobalt(II) from the ferroxidase sites at low concentrations of zinc(II) even though cobalt(II) is present in a large excess over the number of ferroxidase centres.

Table 1
Parameters derived from the potentiometric analysis of metal binding to BFR

Metal ion	pH	Dinuclear centre		Non-specific site	
		K_d (M)	Protons released	K_d (M)	Protons released
Cobalt(II)	5.97	$(1.0 \pm 0.1) \times 10^{-6}$	1.62 ± 0.02	$(2.2 \pm 1.9) \times 10^{-4}$	0.5 ± 0.3
Zinc(II)[a]	5.98	$(1.09 \pm 0.09) \times 10^{-7}$	1.96 ± 0.01	$(7.1 \pm 0.5) \times 10^{-5}$	0.87 ± 0.03
Zinc(II)[b]	6.48	$(2.0 \pm 0.2) \times 10^{-7}$	2.01 ± 0.01	$(1.8 \pm 0.1) \times 10^{-4}$	1.95 ± 0.05

$\mu = 0.1$ M, 25°C.
[a]Site availability 82%.
[b]Site availability 78%.

binding capacity. These data demonstrate that zinc(II) displaced cobalt(II) from the ferroxidase site and is consistent with zinc(II) having a greater binding affinity for the ferroxidase centre than cobalt(II), as the potentiometric data indicate (Fig. 2). However, the fact that the difference spectrum at saturating levels of zinc(II) (e.g. 60 zinc(II) ions per BFR molecule) is not featureless indicates that not all the cobalt(II) is displaced from the protein. However, the difference in maximum metal ion binding capacity does not affect the proton release stoichiometries.

The low-affinity binding sites for zinc(II) and cobalt(II) detected potentiometrically are most probably associated with adventitious binding to the surface of the negatively charged BFR. Further work is required to allow a fuller interpretation of the low-affinity binding stoichiometries, apparent K_d values and metal ion-proton release ratios and since binding at these sites is secondary to binding at the ferroxidase centre we shall not consider it further.

3.3. Charge distribution at the ferroxidase centre of BFR

The X-ray structures of both iron(III)-containing [11] and iron-free R2 subunits of RNR [15] have been reported and no major structural differences found between the two forms. In the apo-form, residues at the dinuclear metal binding site adopt a somewhat altered conformation, in which the hole created by the removal of the iron ions is filled. Thus, in the iron-free protein the four Asp/Glu residues that serve as iron(III) ligands plus an additional Glu are clustered together without compensating charges from metal cations. Åberg et al. [15] present a likely hydrogen-bonding scheme for the centre residues in which the two histidines are protonated and there are an additional two protons associated with the five Asp/Glu residues at pH 6.0. If a similar hydrogen bonding scheme to that seen for apo-RNR were applicable to the metal-free centre of BFR, we envisage the unoccupied centre containing two protonated histidines and two of the four metal ion binding Asp/Glu residues being protonated. In this case the minimum number of protons released for binding of two divalent metal ions should be four. This is close to what is observed at pH 6.0 (Fig. 2) lending support to this description of the BFR dinuclear site. The difference between zinc(II) binding causing the release of ~ 2 protons per ion and cobalt(II) binding causing the release of ~ 1.6 protons per ion may be related to the greater Lewis acidity of zinc(II) and its correspondingly greater effect on the apparent pK_a values of the ligating groups.

An important feature of the dinuclear centre of BFR (Fig. 1) is that when it is occupied by two iron(II) ions in the presence of O_2 the iron(II) becomes oxidised to iron(III) [9]. This could lead to the loss of charge neutrality at the centre. The di-ferric forms of other dinuclear iron proteins contain a bridging O^{2-} ion between the two iron(III) ions which balances the increased positive charge on the metal ions. As yet there have been no reports showing that a similar μ-oxo bridged iron(III) dimer can be formed at the ferroxidase centre of BFR and, given the earlier study of Le Brun et al. [9] which revealed BFR containing 48 iron(III) ions exhibits EPR signals indicative of mononuclear iron, it may be that in this protein such a centre does not form. Therefore, it is interesting to speculate that following formation of a charge compensated di-ferrous centre, the loss of charge compensation within the 4-α-helical bundle as the iron is oxidised to iron(III) leads to the breakdown of the centre. How such a process could be linked to the formation of a non-haem-iron-containing core remains to be determined. This work also points to a further possible role of the ferroxidase centres of BFR, namely, that of a proton channel between the external medium and the internal core space.

Acknowledgements: This work was supported by grants from the BBSRC and EPSRC, who support the UEA Centre for Metalloprotein Spectroscopy and Biology via their Biomolecular Sciences Panel; the EPSRC, whom A.M.K. thanks for the award of a Studentship; the Wellcome Trust, whom N.E.L.B. and G.R.M. thank for a Prize Fellowship and Research Leave Fellowship respectively; the BBSRC, whom S.C.A. thanks for the award of an Advanced Fellowship; NATO, for travel grant 0145/87, which facilitates collaboration between the UEA and UBC laboratories; and the MRC of Canada for grant MT-7182.

References

[1] Warner, R.G. and Weber, I. (1953) J. Am. Chem. Soc 75, 5094–5101.
[2] Tan, A.T. and Woodworth, R.C. (1969) Biochemistry 8, 3711–3716.
[3] Aisen, P. and Harris, D.C. (1989) in: Iron Carriers and Iron Proteins (Loehr, T. ed.) pp. 241–351, VCH, New York.
[4] Watt, G.D., Frankel, R.B. and Papaefthymiou, G.C. (1985) Proc. Natl. Acad. Sci USA 82, 3640–3643.
[5] Yariv, J., Kalb, A.J., Sperling, R., Bauminger, E.R., Cohen, S.G. and Ofer, S. (1981) Biochem. J. 197, 171–175.
[6] Andrews, S.C., Smith, J.M.A., Guest, J.R. and Harrison, P.M. (1989) Biochem. Biophys. Res. Commun. 158, 489–496.
[7] Cheesman, M.R., Thomson, A.J., Greenwood, C., Moore, G.R. and Kadir, F. (1990) Nature 346, 771–773.
[8] Frolow, F., Kalb, A.J. and Yariv, J. (1994) Struct. Biol. 1, 453–460.
[9] Le Brun, N.E., Wilson, M.T., Andrews, S.C., Harrison, P.M., Guest, J.R., Thomson, A.J. and Moore, G.R. (1993) FEBS Lett. 333, 197–202.
[10] Le Brun, N.E., Andrews, S.C., Guest, J.R., Harrison, P.M., Moore, G.R. and Thomson, A.J. (1995) Biochem. J. 312, 385–392.
[11] Nordlund, P., Sjoberg, B.-M. and Eklund, H. (1990) Nature 345, 593–598.

[12] Logan, D.T., Su, X-D., Åberg, A., Regnström, K., Hajdu, J., Eklund, H. and Nordlund, P. (1996) Structure 4, 1053–1064.
[13] Rosenzweig, A.C., Frederick, C.A., Lippard, S.J. and Nordlund, P. (1993) Nature 366, 537–543.
[14] Keech, A.M., Le Brun, N.E., Wilson, M.T., Andrews, S.C., Moore, G.R. and Thomson, A.J. (1996) J. Biol. Chem. (in press).
[15] Åberg, A., Nordlund, P. and Eklund, H. (1993) Nature 361, 276–278.
[16] Bauminger, E.R., Harrison, P.M., Hechel, D., Nowik, I. and Treffry, A. (1991) Biochim. Biophys. Acta 1118, 48–58
[17] Falk, J.E. (1964) in: Porphyrins and Metalloporphyrins, BBA Library vol. 2, pp. 181–182, Elsevier/North-Holland, Amsterdam.
[18] Laskowski, M., Jr. and Finkenstadt, W.R. (1972) Methods Enzymol. 26, 193–277.
[19] Mauk, M.R., Parker, P.D. and Mauk, A.G. (1991) Biochemistry 30, 9873–9881.
[20] Mauk, M.R., Ferrer, J.C. and Mauk, A.G. (1994) Biochemistry 33, 12609–12614.